



Characterization of QCM sensor surfaces coated with molecularly imprinted nanoparticles

Kristina Reimhult^a, Keiichi Yoshimatsu^b, Klas Risveden^b, Si Chen^a,
Lei Ye^b, Anatol Krozer^{a,*}

^a The IMEGO Institute, Arvid Hedvalls Backe 4, SE-411 33 Göteborg, Sweden

^b Pure and Applied Biochemistry, Chemical Center, Lund University, Box 124, SE-221 00 Lund, Sweden

ARTICLE INFO

Article history:

Received 23 November 2007

Received in revised form 30 January 2008

Accepted 6 February 2008

Available online 17 February 2008

Keywords:

Molecularly imprinted polymers

Quartz crystal microbalance

Nanoparticles

Sensors

ABSTRACT

Molecularly imprinted polymers (MIPs) are gaining great interest as tailor-made recognition materials for the development of biomimetic sensors. Various approaches have been adopted to interface MIPs with different transducers, including the use of pre-made imprinted particles and the *in situ* preparation of thin polymer layers directly on transducer surfaces. In this work we functionalized quartz crystal microbalance (QCM) sensor crystals by coating the sensing surfaces with pre-made molecularly imprinted nanoparticles. The nanoparticles were immobilized on the QCM transducers by physical entrapment in a thin poly(ethylene terephthalate) (PET) layer that was spin-coated on the transducer surface. By controlling the deposition conditions, it was possible to gain a high nanoparticle loading in a stable PET layer, allowing the recognition sites in nanoparticles to be easily accessed by the test analytes. In this work, different sensor surfaces were studied by micro-profilometry and atomic force microscopy and the functionality was evaluated using quartz crystal microbalance with dissipation (QCM-D). The molecular recognition capability of the sensors were also confirmed using radioligand binding analysis by testing their response to the presence of the test compounds, (R)- and (S)-propranolol in aqueous buffer.

© 2008 Elsevier B.V. All rights reserved.

1. Introduction

In biomimetic sensors, stable synthetic recognition materials are used to replace biological macromolecules (antibodies, enzymes, membrane receptors, aptamers) and whole cells to provide a high molecular recognition selectivity. Because of the high stability of synthetic recognition materials, biomimetic sensors have great potential in applications where biosensors are found difficult to use, for example for in-field use and under harsh conditions. Molecularly imprinted polymers (MIPs) are cross-linked organic structures containing pre-designed molecular recognition sites. MIPs are produced by template-directed polymerization, in which the formation of the recognition sites is controlled by the specific molecular interactions between a template and appropriate functional monomers (Sellergren, 2001; Komiyama et al., 2003; Yan and Ramström, 2005). Traditional MIPs are prepared as porous monoliths that after a series of grinding and fragmentation steps results in a sample of irregular particles. Although use of irregular MIP particles as recognition materials to develop biomimetic sensors has been reported in the literature (Alexander et al., 2006), the

methods used for immobilization of MIP particles on transducers remain largely unexplored. Besides using pre-made MIP particles, another approach of producing MIP-based sensors is to prepare a thin imprinted polymer layer directly on the transducer surface (Piacham et al., 2005; Li and Husson, 2006). The advantage of the *in situ* MIP preparation method is that the thickness of the MIP layer can be well controlled by means of surface initiated polymerization and living radical polymerization techniques. It is well known that many sensing principles, e.g. surface plasma resonance (SPR), require the thickness of the MIP layer to be less than about 100 nm, because any binding event occurring beyond this distance from the transducer surface cannot generate a detectable signal.

The difficulty of the *in situ* preparation method is that often an *ex situ* optimized MIP preparation condition described in the literature cannot be applied under the *in situ* condition, which makes the *in situ* MIP performance compromised. Another shortcoming of *in situ* preparation is the difficulty to integrate MIPs against several different target molecules with transducers in an array format. The preparation of MIP functionalized array transducers is much easier when attaching pre-made imprinted particles on a sensor substrate.

The advancement in production of nano-sized MIP particles provides a new opportunity to use pre-made MIPs to fabricate thin recognition layers on transducers. Given that high quality MIP

* Corresponding author. Tel.: +46 31 750 18 06; fax: +46 31 750 18 01.
E-mail address: Anatol.Krozer@imego.com (A. Krozer).

nanoparticles can be easily synthesized using emulsion and precipitation polymerization (Priego-Capote et al., *in press*; Yoshimatsu et al., 2007), they can be used as a basic building block to assemble a recognition layer on a transducer surface, either by direct chemical coupling (Ye et al., 2001) or through immobilization in a thin polymer layer deposited on a transducer surface (Surugiu et al., 2001). In this work we studied the latter preparation method applied to a quartz crystal microbalance (QCM) transducer surface, and characterized the MIP layer using a profilometer and atomic force microscopy (AFM) (Binnig et al., 1986). Quartz crystal microbalance with dissipation (QCM-D) was used as the detection method for evaluating the function of the MIP layer. The QCM technique has been frequently applied to analyte detection of imprinted polymers in the past (Sallacan et al., 2002; Piacham et al., 2005). In addition, QCM-D not only provides frequency change as an approximate indication for mass accumulation caused by analyte binding, but also gives information of energy dissipation that reflects the change of viscoelastic properties accompanying analyte binding (Höök and Rudh, 2005; Geelhood et al., 2002; Höök et al., 1997). For sensor functionalization, MIP nanoparticles were dispersed in a poly(ethylene terephthalate) (PET) solution and spin-coated on the QCM surface. The sensing layer has very good stability and could be used repeatedly after different regeneration treatments. Our two main purposes were to study if deposition of MIP nanoparticles in a supporting polymer film can be used as a generic approach to assemble biomimetic sensors, and further to apply gravimetry using the QCM-D technique to characterize the uptake and desorption kinetics of such films.

2. Experimental

2.1. Materials

Trimethylolpropane trimethacrylate (TRIM, technical grade) was obtained from Aldrich (Dorset, U.K.). Acetonitrile (99.7%) and azobisisobutyronitrile (AIBN, 98%) used for nanoparticle synthesis were purchased from Merck (Darmstadt, Germany). AIBN was re-crystallized from methanol before use. Methacrylic acid (MAA, 98.5%) was purchased from ACROS (Geel, Belgium) and used as received. (*R*)-Propranolol hydrochloride and (*S*)-propranolol hydrochloride (99%) were supplied by Fluka (Dorset, U.K.). (*S*)-[4-³H]-Propranolol (specific activity 555 GBq mmol⁻¹, 66.7 μM solution in ethanol) was purchased from NEN Life Science Products Inc. (Boston, MA). Scintillation liquid, Ecoscint A was obtained from National Diagnostics (Atlanta, GA). Trisodium citrate dihydrate was purchased from Sigma–Aldrich, citric acid monohydrate (reagent grade, 99.5%) and ethanol (analytical grade, 96%) for the QCM-D experiments were purchased from GTF Fisher (Gothenburg, Sweden). For synthesis of imprinted nanoparticles, (*R*)-propranolol hydrochloride and (*S*)-propranolol hydrochloride were converted into free base form before use. PET was purchased from Wellman International Ltd. (Ireland). Analytical grade trifluoroacetic acid (TFA) and dichloromethane (DCM) were obtained from Aldrich (Dorset, U.K.) and used without further purification. Other solvents were of analytical grade.

2.2. Apparatus

The quartz crystal microbalance with dissipation system Q-Sense D300 (Q-Sense AB, Västra Frölunda, Sweden) was used with AT-cut gold-coated quartz crystals (Ø 14 mm) with a resonance frequency of 5 MHz as the sensing elements. For nanoparticle deposition, a spin coater (Model 5700, Precision Spin Coating Systems, USA) was used. For measurement of film thickness, a Tencor Alpha Step 500 surface profilometer was used. Detailed surface topog-

raphy of the nanoparticle coatings was observed using an AFM with an NTEGRA-Configuration: NTEGRA-BIO-SNOM-EC in Resonant Mode (NT-MDT, Russia). The AFM tips used were non-contact “Golden” silicon cantilevers (NSG 11) tips with a typical curvature radius = 10 nm, a cone angle $f \leq 22^\circ$ and a force constant ≈ 5.5 N/m (NT-MDT). Radioactivity was measured using a model 1219 Rack-beta β -radiation counter from LKB Wallac (Solentuna, Sweden).

2.3. Synthesis of molecularly imprinted nanoparticles

Molecularly imprinted nanoparticles were synthesized using a precipitation polymerization method described in a previous publication (Yoshimatsu et al., 2007). Briefly, the template molecule, (*S*)- or (*R*)-propranolol in its free base form (137 mg, 0.53 mmol) was dissolved in 40 ml of acetonitrile in a 150 mm × 25 mm borosilicate glass tube equipped with a screw cap. MAA (113 mg, 1.31 mmol), TRIM (684 mg, 2.02 mmol) and AIBN (28 mg, 3 wt% of monomer) were then added. The solution was purged with a gentle flow of argon for 5 min and sealed under argon. Polymerization was carried out by inserting the borosilicate glass tube in a water bath pre-set at 60 °C for 24 h. After polymerization, particles were collected by centrifugation at 18,000 rpm (38,000 × *g*) for 20 min. The template was removed by batch-mode solvent extraction with methanol containing 10% acetic acid (v/v), until no template could be detected from the washing solvent by spectrometric measurement (UV 290 nm). Polymer particles were finally washed with acetone and dried in a vacuum chamber. The resulting MIP particles, MIP(*S*) and MIP(*R*), were imprinted against (*S*)- or (*R*)-propranolol respectively. Non-imprinted reference polymers, NIP, were synthesized under identical conditions except for omission of the template.

2.4. Radioligand binding analysis

In a series of polypropylene microcentrifuge tubes, increasing amounts of polymer particles were suspended in 1 ml of a 50:50 (v/v) mixture of 25 mM citrate buffer (pH 6.0):acetonitrile (citrate/MeCN). After addition of (*S*)-[4-³H]-propranolol (246 fmol to 1 ml polymer solution), the mixtures were incubated at room temperature overnight. A rocking table was used to provide gentle mixing. After the incubation, samples were centrifuged at 14,000 rpm for 10 min. Supernatant (500 μl) was taken from each microcentrifuge tube and mixed with 10 ml of scintillation liquid (Ecoscint A), from which the radioactivity was measured. The amount of labeled (*S*)-propranolol bound to polymer particles was calculated by subtraction of the free fraction from the total amount added. Data are mean values of duplicate measurements.

In competitive radioligand binding experiments, (*S*)-[4-³H]-propranolol (246 fmol) was incubated with a fixed amount of nanoparticles in the presence of excess non-labeled (*S*)- or (*R*)-propranolol hydrochloride. After centrifugation, samples were treated with the same procedure as described above.

2.5. Preparation of nanoparticle-coated QCM resonator wafers

The QCM resonator wafers (Ø 14 mm, gold coated) were cleaned in a 1:1:5 (v/v) mixture of H₂O₂ (30%):ammonia (25%):purified water heated at 75 °C for 5 min, rinsed with copious amounts of purified water and blown dry with a gentle flow of nitrogen. Polymer nanoparticles were suspended in a solution of 1 wt% PET in a 50:50 (v/v) mixture of DCM:TFA. The nanoparticle concentration in the final mixture was fixed at 0.2 wt% and 2 wt% (Table 1). After a brief ultrasound sonication, 80 μl of the suspension was dispensed onto the gold-coated QCM resonator, which was spun at 2000 rpm for 30 s. After spin-coating, the QCM resonator was kept in a vacuum chamber overnight.

Table 1
Measurement of film thickness on QCM sensors with profilometer

QCM sensor	Nanoparticles coated	Nanoparticle content (%)	Step height (mm, location 1)	Step height (mm, location 2)
QCM(S)-1	MIP(S)	0.2	280 ± 40	250 ± 35
QCM(R)-1	MIP(R)	0.2	280 ± 100	240 ± 50
QCM(S)-2	MIP(S)	2	600 ± 55	490 ± 50
QCM(R)-2	MIP(R)	2	500 ± 45	630 ± 85

2.6. Characterization of nanoparticle coating with AFM

The surface topography of the QCM sensor chips was studied using AFM at 23 °C, in 50% relative humidity. Precautions were taken not to bring the cantilever of the AFM in contact with the surface using the AFM in semi-contact mode. The surface topographies of the coatings were acquired without any distortion of the QCM sensor chips surfaces. Non-destructive surface topography investigations of spin-coated polymer layers on sensor chip surfaces using AFM in semi-contact mode have earlier been reported (Risveden et al., 2007a,b). To avoid electrostatic interactions, the QCM chips were grounded during imaging.

2.7. Responses of MIP-coated QCM wafers to (S)- and (R)-propranolol

All QCM-D experiments reported here were carried out in a 25 mM citrate buffer (pH 6.0) containing 5% ethanol (v/v) (citrate/EtOH) at 23 °C (±0.05 °C), with the temperature being controlled by the instrument. The experiments were performed by sudden exchange of the solutions in the experimental chamber without further recirculation. One typically exposed the sensor surface to pure buffer or buffer containing the analyte and monitored the time response of the sensor. The sensor response was, most probably, mass transport limited and did not describe the true reaction kinetics.

Between each new propranolol addition the MIP-coated quartz crystal surface was regenerated by several rinsing steps with the citrate/EtOH buffer. The rinsing proceeded until a stable baseline was obtained at a value close to the one observed prior to propranolol exposure. The changes in the resonance frequency (ΔF) and the energy dissipation (ΔD) caused by the analyte binding, were all simultaneously recorded for the fundamental frequency and the first three overtones.

The simplified relation between the shift in frequency (ΔF) and the mass of the adsorbed layer (Δm) is described by the Sauerbrey relation (Sauerbrey, 1959):

$$\Delta m = \frac{-C \Delta F_n}{n} \quad (1)$$

where C is the mass sensitivity constant ($C = 17.7 \text{ ng cm}^{-2} \text{ Hz}^{-1}$ for a 5 MHz crystal), $n = 1$ for the fundamental frequency and $n > 1$ is the overtone number ($n = 3, 5, \dots$). All data presented are collected from the first overtone with values for the frequency divided by three ($\Delta F_3/3$). The dissipation, D , is given by $D = 1/\pi F_{\text{res}} \tau$, where τ is the decay time constant of the loaded quartz and F_{res} is its resonance frequency. Both τ and F_{res} are determined when the wafer is oscillating freely after it has been disconnected from the driving electronics.

Several analyte exposures and measurements of the corresponding absorption and desorption behaviour have been performed on each nanoparticle-coated wafer. The results presented in this article stem from six different quartz wafers covered with MIP(S), MIP(R) or NIP nanospheres (two quartz wafers of each type) at four different occasions.

3. Results and discussion

3.1. Confirmation of chiral selective analyte binding with imprinted nanoparticles

In this work, preparation of imprinted nanoparticles was carried out using an optimized precipitation polymerization protocol (Yoshimatsu et al., 2007), except that a pure enantiomer, (S)- or (R)-propranolol was used as the template. In this way two different types of imprinted nanoparticles, MIP(S) and MIP(R) were obtained, which contains specific sites preferentially for (S)- and (R)-propranolol, respectively. The average size of the imprinted nanoparticles in the dry state is 130 nm with a narrow size distribution, as measured by scanning electron microscopy. When the nanoparticles were dispersed in neat acetonitrile, they have a mean hydrodynamic radius of approximately 100 nm as measured by dynamic light scattering (Yoshimatsu et al., 2007). On average, the non-imprinted nanoparticles are two times larger than the imprinted nanoparticles, which can be attributed to the fact that the template used during the polymerization has an important effect on the particle nucleation and growth.

To confirm the imprinting effect, the (S)- and (R)-propranolol-imprinted nanoparticles (MIP(S) and MIP(R)) were incubated with a fixed amount of [^3H]-(*S*)-propranolol in citrate/MeCN. The ratio of the radioligand bound to the nanoparticles relative to the total amount was shown in Fig. 1. As seen, the (S)-imprinted nanoparticles bind the labeled (S)-propranolol much more effectively than the (R)-imprinted nanoparticles, indicating that the chiral structure of the template has been successfully imprinted in the nanoparticles' recognition sites. Compared to non-imprinted nanoparticles that showed almost no propranolol binding at a polymer concentration as high as 2 mg/ml (Fig. 1), the (R)-imprinted nanoparticles could bind also the labeled (S)-ligand. This indicates that the chiral imprinted sites indeed have certain cross-reactivity towards the "wrong" enantiomer. For a more quantitative measure, at polymer concentration of 0.125 mg/ml, the amount of labeled (S)-ligand bound to MIP(S) was two times of that bound to MIP(R).

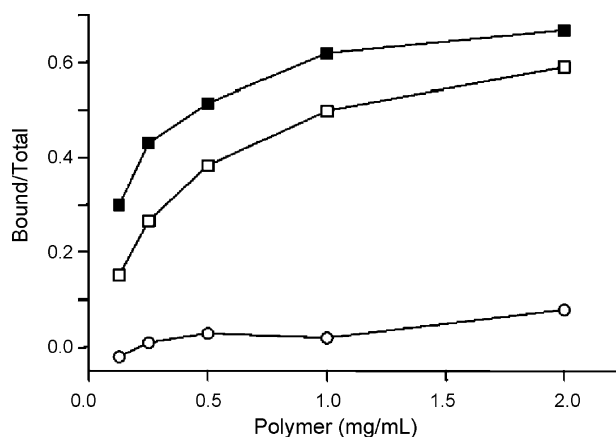


Fig. 1. Uptake of [^3H]-(*S*)-propranolol with different amount of MIP(S) (■), MIP(R) (□) and NIP (○) in 25 mM citrate buffer (pH 6.0)/acetonitrile (50/50, v/v). Initial concentration of the labeled ligand: 0.246 nM.

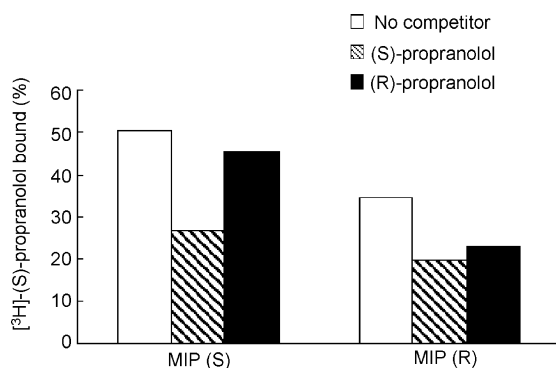


Fig. 2. Displacement of labeled (S)-propranolol bound to the imprinted nanoparticles with excess non-labeled (S)- and (R)-propranolol. Solvent: 25 mM citrate buffer (pH 6.0)/acetonitrile (50/50, v/v), nanoparticle concentration: 0.44 mg/ml, initial concentration of [^3H]- (S)-propranolol: 0.246 nM, initial concentration of the competing (S)- and (R)-propranolol: 2.86 μM .

The presence of the high fidelity chiral sites can also be appreciated by looking at the displacement experimental results (Fig. 2). For MIP(S), non-labeled (S)-propranolol could displace 46% of the labeled (S)-ligand that originally bound to the polymer, whereas non-labeled (R)-propranolol only gave 10% displacement. This is because the labeled and non-labeled (S)-propranolol have the same chemical structure, therefore the non-labeled (S)-propranolol can effectively compete with the labeled (S)-propranolol for the limited number of chiral sites. On the other hand, with MIP(R), the 33% labeled (S)-ligand bound in the absence of competitor was located in non-selective sites, therefore it can be equally displaced by both the non-labeled (S)- and (R)-propranolol. The results obtained from these radioligand binding analyses suggest the following: (1) by molecular imprinting, chiral selective recognition sites are generated in nanoparticles; (2) effective chiral selective ligand displacement takes place only in the chiral selective sites of the imprinted nanoparticles.

It is instructive to evaluate the binding conditions for the radioligand experiments shown in Figs. 1 and 2 for subsequent comparison with the measurements on coated surfaces using the QCM-D technique. The solutions used for radioligand binding detection contained approximately 9×10^{11} imprinted nanoparticles (1 mg/ml MIP in 1 ml sample, diameter 130 nm (Yoshimatsu et al., 2007) and assumed density of the MIP particles same as for water). The imprinted nanoparticles were exposed to solutions containing 246 fmol of propranolol, which results in a nanoparticle to analyte ratio of roughly 6:1. The radioligand binding analysis is an extremely sensitive technique, allowing a small amount of the very best binding sites to be studied. In comparison, in the QCM-D experiments the nanoparticle:analyte ratio was much lower (see Section 3.4), making the majority of binding events to take place at sites of much lower fidelity, which can lead to sensor responses of lowered chiral selectivity.

3.2. Use of imprinted nanoparticles as building blocks for sensor fabrication

The outstanding molecular recognition capability and the small physical size of imprinted nanoparticles make them attractive for use as building blocks to fabricate new biomimetic sensors. As mentioned earlier, to get the maximum response from a specific binding event, recognition layers on many transducer surfaces have to be restricted. While *in situ* MIP preparation can afford thin polymer layers, the obtained imprinted polymers have so far showed only moderate success. One problem is that often there is a trade off between the control of film thickness and the use of optimal imprinting condition, resulting in a poor imprinting effect of the

thin *in situ* prepared layers. For example, atom transfer radical polymerization (ATRP) is a powerful technique to prepare thin polymer film on solid surface, however, it cannot be used as a general method to coat MIP layer, because the commonly used functional monomers and templates can disrupt the critical Cu(I)-ligand complex used to catalyze the polymerization (Li and Husson, 2006). Provided that imprinted nanoparticles can be readily synthesized, it should be possible to use these nanoparticles as building blocks to assemble thin molecular recognition layer. In this way one can guarantee that high quality MIPs are utilized to gain the best selectivity.

Nanoparticle self-assembly is one obvious approach for deposition of MIPs on transducer surface. However, given that practical sensors need to be stable for repeated uses and can stand relatively harsh regeneration steps, we need to design an approach that can firmly keep MIP nanoparticles in place. We therefore choose to use an inert supporting polymer, PET, to anchor nanoparticles on the surface. The good solvent resistance of PET allows the sensor surface to be used in both aqueous environment and in most commonly used organic solvents (acetonitrile, ethanol, etc.). In previous studies, we have found that when imprinted nanoparticles were encapsulated in PET nanofibers, their molecular recognition sites remained easily accessible for template binding (Chronakis et al., 2006). This prompted us to use PET as supporting matrix to immobilize MIP nanoparticles on the present QCM resonator. With spin coating, it was easy to adjust the final thickness of spin-coated MIP layer by changing the total solid content (PET and nanoparticles) and the ratio between nanoparticles and PET. After optimization, we could get very thin (<1 μm) MIP nanoparticle coatings by using the following suspension: 1 wt% PET, 0.2–2 wt% nanoparticles in DCM/TFA (50/50, v/v). Supposing the spinning process does not alter the nanoparticle/PET ratio, we got on the sensor surface a layer of polymer coating containing 17–67% MIP nanoparticles. When tested in several different solvents, it was found that all the sensor surfaces remained very stable, no peeling off of the film or particle loss was observed. Nor was the layer affected by several weeks of exposure to citrate/EtOH buffer. To measure the thickness of the MIP coating, part of the coated layer was removed with a razor before the surface was scanned with a profilometer. The mean step heights measured with the profilometer for the different sensor surfaces are given in Table 1. As seen, with higher nanoparticle loading (67%), thicker films (490–630 nm) are obtained, which indicates a multilayer particle film. A low nanoparticle loading (17%) led to a thin MIP nanoparticle coating (240–280 nm).

3.3. Characterization of MIP nanoparticle coatings with AFM

To get more detailed structural information about the nanoparticle coating, we used AFM to study the surface profiles on the different sensor surfaces. At the onset of our experiments, we used AFM to scan over the step section on one of the QCM sensor surfaces (QCM(S)-1) that has been measured by profilometer. Within the scanned area, the nanoparticle coating was relatively uniform, and the step height was approximately 200 nm, indicating close to monolayer coverage of the samples coated with 0.2% nanoparticle solution and supporting the profilometer data shown in Table 1. A large area scan, $70 \mu\text{m} \times 70 \mu\text{m}$ (Supporting Information) confirmed the uniformity of the covering film.

Fig. 3 shows the local AFM scans over a $2 \mu\text{m} \times 2 \mu\text{m}$ area on each QCM sensor. While on all the sensor surfaces nanoparticles were found well distributed, the 10-fold increase (to 2%) in nanoparticle loading investigated in the spin-coating step resulted in thicker (Table 1) and more even (Fig. 3) nanoparticle coverage. For all nanoparticle-coated sensors, the observed dot size under AFM matches the size of the nanoparticles as obtained by scanning electron microscopy. Fig. 3 also shows the clear difference between

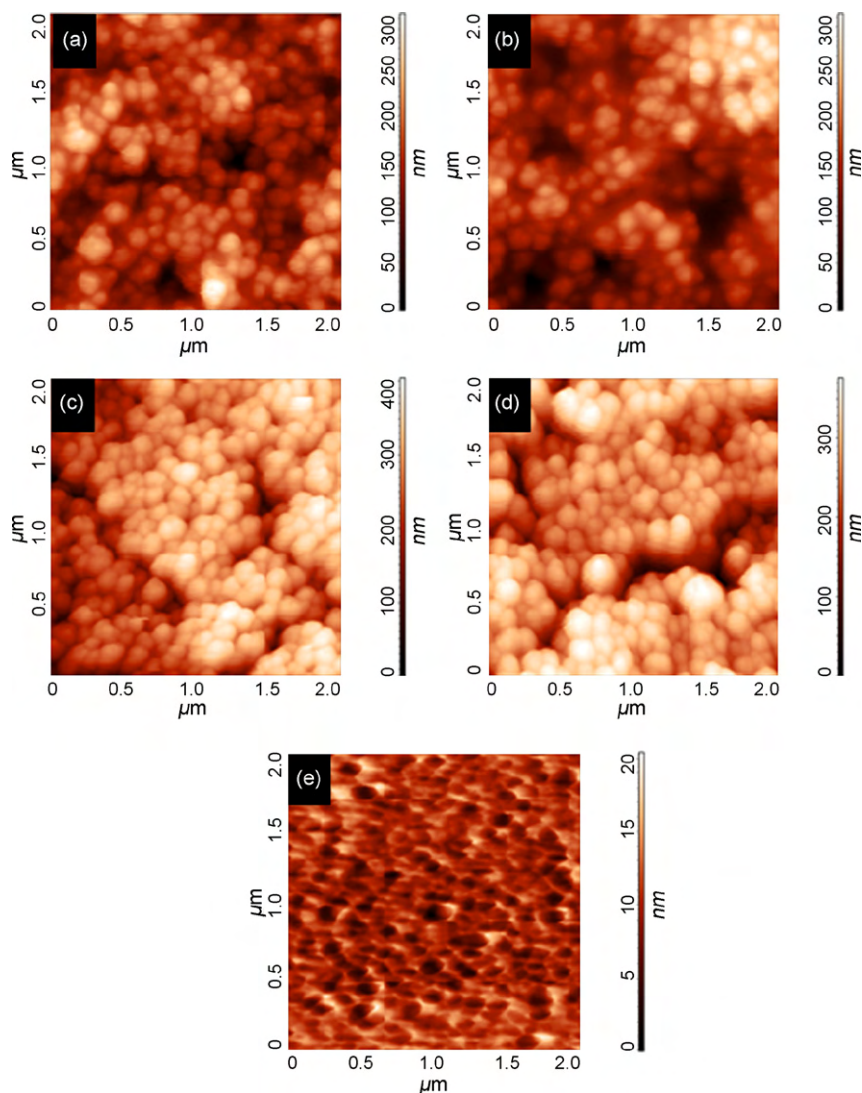


Fig. 3. AFM images of QCM(S)-1 (a), QCM(R)-1 (b), QCM(S)-2 (c), QCM(R)-2 (d) and uncoated QCM gold surface (e). The AFM scan speeds were $1.72 \mu\text{m/s}$ (a, d and e) and $1.70 \mu\text{m/s}$ (b and c). Note the different color scale used for the bare gold surface.

uncoated and nanoparticle-coated surfaces, with coated sensors having a rough surface compared to the gold-plated QCM resonator. The average roughness (R_a) of QCM(S)-1, QCM(R)-1, QCM(S)-2 and QCM(R)-2 are 33.9 nm, 40.3 nm, 52.6 nm and 43.6 nm, respectively. For comparison, the R_a of the bare gold surface is 1.9 nm.

3.4. Response of MIP nanoparticle-coated QCM sensors

As mentioned in Section 2.7 the response of nanoparticle-coated QCM sensor surfaces were tested in aqueous citrate buffer containing 5% ethanol, with the small portion of ethanol added to improve solvent contact to the relatively hydrophobic coating. In all QCM experiments presented in this article the 2% nanoparticle loading was used. Although we report here the results only from the uptakes of propranolol dissolved in the citrate/EtOH buffer, the crystals used were also evaluated in a similar series of experiments using a 50:50 (v/v) mixture of 25 mM citrate buffer (pH 6.0) and acetonitrile.

Apart from the response to mass changes the quartz microbalance response in solution is known to be affected by three parameters: the fluid density and viscosity as well as by the temperature. The temperature was kept constant (see Section 2.7). Since we used an aqueous buffer containing ethanol and since it

is well known that ethanol is volatile, it was important to ensure that the signal contribution due to possible variation in ethanol concentration would be negligible for a given set of experiments. Therefore we have calibrated the response of the MIP-coated wafers to buffers with slightly different ethanol concentrations. From evaporation experiments we estimate the maximum variation of ethanol concentration during a single set of experiments to be $<0.5\%$. The calibration experiments gave shifts of 4 Hz in frequency and 2×10^{-6} in dissipation per percentage point change in ethanol composition, therefore the resulting uncertainty due to evaporation can be considered negligible except for the lowest propranolol concentration tested (data not shown).

Fig. 4 shows typical results on adsorption and desorption kinetics obtained on one of the wafers covered by nanoparticles imprinted against (*R*)-Propranolol (MIP(*R*)) dispersed in PET and sequentially exposed to varying concentrations of (*R*)- and (*S*)-propranolol in citrate/EtOH buffer, respectively. Both the frequency response and the dissipation are shown for the 3rd harmonics. This particular quartz wafer does not exhibit any chiral recognition, which is due to the fact that the sample previously had been exposed to citrate/MeCN solutions. We will discuss this point in more detail below.

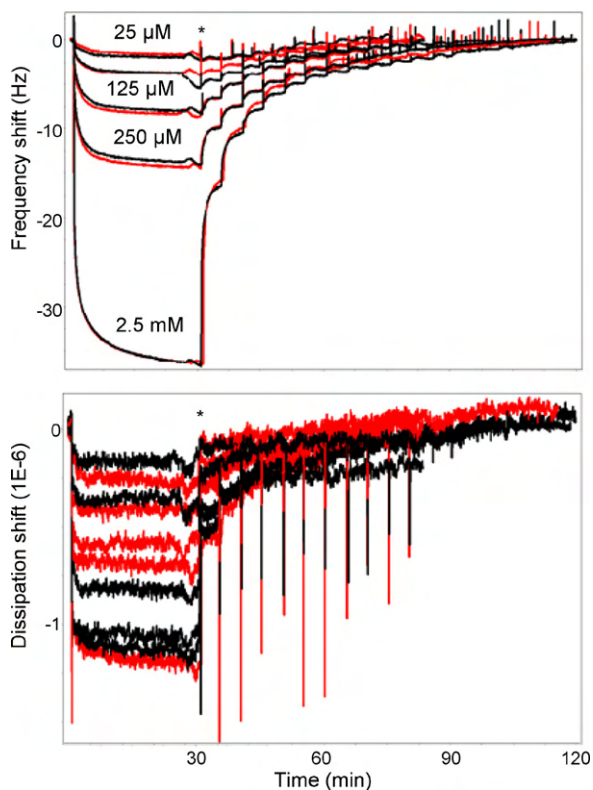


Fig. 4. The kinetics of propranolol adsorption and desorption of MIP(R) after MeCN exposure. * indicates the start of the rinsing with buffer. The results for both (R)- and (S)-propranolol are shown (black and red, respectively) for the 3rd harmonics. The frequency results are given as $\Delta F_3/3$. Note that the dissipation curves and the 50 μM frequency curve have no labels due to lack of space.

As can be seen from the presented data the detection limit of the set up to propranolol is about 10 μM . Using Eq. (1) and the known molecular weight of propranolol we obtain that the highest uptake shown in Fig. 4 (for 2.5 mM propranolol) corresponds to approximately 2 nmol/cm² or about 1×10^{15} molecules/cm². The profilometer data in Table 1 indicates a coverage of at most four monolayers for the samples prepared using 2% nanoparticle solutions. A single close-packed layer of nanoparticles contains approximately 8×10^9 particles/cm². Therefore the nanoparticle to propranolol ratio for this QCM-D experiment is about 1:37,500 as compared to 6:1 in the radioligand binding experiments, meaning that we probe vastly different propranolol sites in the two types of experiments. Estimating the binding efficiency of the MIP particles to 0.1 wt% and using assumptions already mentioned, one MIP particle should be able to accommodate about 2500 propranolol molecules. It is then clear that a single particle is unable to accommodate large number of analytes as the achieved 37,500—either the non-specific adsorption is substantial, or else the signal we detect stems not from the mass increase associated with the bound propranolol molecules, but is due to other phenomena, such as swelling of the polymer film and incorporation of extra solvent in the film upon propranolol binding.

The frequency and the dissipation changes in Fig. 4 did not show the same trend. Whereas the magnitude of the frequency shift increased monotonically with increasing propranolol concentration, the dissipation shift did not, and was also somewhat different for the different enantiomers.

The kinetics of the frequency data in Fig. 4 did not fit simple Langmuir kinetics, neither for the uptake nor for the desorption phase. This is not surprising. Usually molecular imprints contain

sites with a broad distribution of target binding energies which usually also have different geometric accessibility to an analyte molecule. If the adsorption onto different sites proceeds independently from each other one would at simplest expect the analyte to obey several different Langmuir kinetics. In addition the kinetics can be limited by the analyte mass transport or by steric effects. An example of fitting of the experimental data to two Langmuir-like distributions is given in the Supporting Information.

Fig. 5 summarizes the frequency and dissipation shifts corresponding to uptake of the MIP(R) and NIP samples exposed to (R)- and (S)-propranolol in citrate/EtOH solutions, respectively. Shown are not the shifts after reaching saturation uptake but the uptake data after 10 min of exposure to propranolol. Qualitatively the trends were similar for the MIP(S) samples (Supporting Information) except for the dissipation prior to exposure to MeCN. The dissipation shifts of the MIP(S) samples upon analyte exposure were negligible. There is a substantial data spread in the plots in Fig. 5, and the data spread is larger for samples prior to their exposure to citrate buffer containing acetonitrile. As can be seen in Fig. 5 there is a difference in template binding between non-imprinted and imprinted nanoparticles, indicating a functionality of the imprinted particles. The MIP(R) propranolol uptake, represented by the frequency shift, is considerably smaller prior to the sample exposure to citrate/MeCN than after, but the MIP(R) do show a degree of chiral recognition and discrimination between (R)- and (S)-propranolol before exposure to citrate/MeCN. As can be seen by comparing the data for non-imprinted polymers before and after citrate/MeCN exposure, Fig. 5 shows that the non-specific binding is substantially lower for samples before their exposure to citrate/MeCN solutions. It may be that the lower non-specific binding of the MIP(R) samples before citrate/MeCN exposure enables the chirality to appear more clearly. We should note that the chiral selectivity of the MIP(R)-coated QCM sensor is rather limited since the QCM measurement was carried out at an analyte concentration of at least 0.25 mM that saturated the sensor surface. The need to use relatively high propranolol concentrations is due to the high analyte detection limit of the QCM technique when used together with MIP systems. Our present detection limit in buffer (10 μM) is similar to that obtained previously with a thicker MIP layer (2 μm) applied in pure organic solvent (Haupt et al., 1999), however the response time of our present sensor is much shorter (less than 5 min).

A notable feature is the relatively large increase of dissipation upon (R)-propranolol binding of the MIP(R) samples prior to exposure to citrate/MeCN solutions. Considering the dissipation shifts it is clear that (R)-propranolol solutions affect the MIP(R) far more than (S)-propranolol do, and the effect of (R)-propranolol on MIP(R) is much stronger than on NIP. The chiral selectivity of MIP(R) is shown more clearly when taking not only the frequency shift but also the dissipation shift into account. The dissipation shifts of the samples were positive prior to exposure to citrate/MeCN, while after the exposure the shifts were low but negative. The former implies that the film gets softer upon analyte binding while the latter implies that it becomes somewhat stiffer (Voinova et al., 1997). This is a clear indication that the MeCN exposure drastically changes the performance of the samples.

A possible explanation to the observed difference in analyte binding before and after citrate/MeCN exposure is that the acetonitrile penetrates the porous polymer and becomes bound inside the pores much like crystal water may. This would suggest that after exposure of the samples to solutions containing acetonitrile further experiments take place in its presence. Previous reports have concluded that the citrate/MeCN buffers appear to be superior with respect to chirally specific recognition and the magnitude of non-specific binding (Yoshimatsu et al., 2007; Ye et al., 2002),

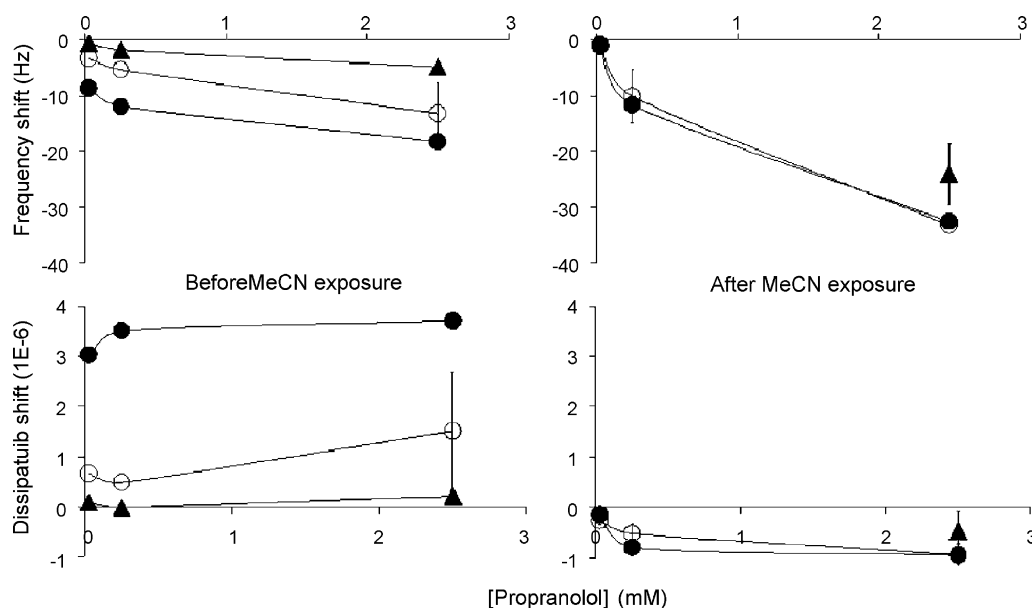


Fig. 5. Shifts in frequency and dissipation when adding (*R*)-propranolol (●) and (*S*)-propranolol (○) to MIP(*R*), and (*R*)- or (*S*)-propranolol to NIP (▲) before and after the coated QCM wafers have been exposed to citrate/MeCN solutions, respectively. Data are collected in a 25 mM citrate buffer (pH 6.0) containing 5% ethanol (v/v). Data are shown for the 3rd harmonics, with the frequency results given as $\Delta F_3/3$.

yet the performance in citrate/EtOH of the imprinted nanospheres deposited in PET onto the surfaces seems to deteriorate after the citrate/MeCN exposures. This could be due to MeCN affecting the PET matrix. Measurements on only PET covered substrates before and after MeCN exposure have shown that the deposited film became heavier, but that the adsorption of propranolol to PET is unchanged and low (Supporting Information). Fig. 5 shows that the dissipation of the films exposed to citrate/MeCN upon analyte binding is very different from the dissipation of the films prior to their exposure to citrate/MeCN. This suggests that irreversible mechanical changes of the MIP-including PET film, such as stiffness changes or volume changes, may have taken place during MeCN exposure. Since the surface bound nanoparticles are embedded into and possibly constricted by the PET matrix, changes of this matrix may change the signal transduction upon molecular recognition events.

4. Conclusion

In this work we investigated a new and generic approach for integration of molecularly imprinted nanoparticles into sensing systems. As demonstrated, nanoparticles can be easily immobilized on flat transducer surfaces through a supporting polymer film using spin-coating, and the thickness of the nanoparticle coating can be easily controlled by changing the nanoparticle/polymer ratio and the solid content of the nanoparticle suspension. AFM showed to be a convenient tool to study the nanoparticle surface distribution in the polymer film on the QCM-D sensor chip. With QCM-D sensors coated with MIP nanoparticles, a moderate chiral selectivity was achieved. The limited chiral selectivity can partly be explained by high non-specific binding resulting from the high analyte concentrations required for the QCM-D measurements. QCM-D probes also mechanical properties of the resulting complex surface film (particles embedded into a polymer matrix) which seems to be important for the molecular recognition and gives valuable information of the binding process. We have further shown that it is imperative to use appropriate buffers and these may be different when evaluating embedded particles on surfaces as compared to optimal buffers for

free particles in solution. More importantly, this work has shown that MIP nanoparticles can indeed be used as building blocks to prepare more complex structures and devices. Further work on combining MIP nanoparticles with more sensitive transducers for biomimetic sensor development is on going.

Appendix A. Supplementary data

Supplementary data associated with this article can be found, in the online version, at doi:10.1016/j.bios.2008.02.011.

References

- Alexander, C., Andersson, H.S., Andersson, L.I., Ansell, R.J., Kirsh, N., Nicholls, I.A., O'Mahony, J., Whitcombe, M.J., 2006. *J. Mol. Recogn.* 19, 106–180.
- Binnig, G., Quate, C.F., Gerber, C., 1986. *Phys. Rev. Lett.* 56, 930–933.
- Chronakis, I.S., Jakob, A., Hagström, B., Ye, L., 2006. *Langmuir* 22, 8960–8965.
- Geelhoed, S.J., Frank, C.W., Kanazawa, K., 2002. *J. Electrochem. Soc.* 149, H33–H38.
- Haupt, K., Noworyta, K., Kutner, W., 1999. *Anal. Commun.* 36 (11/12), 391–393.
- Höök, F., Rudh, M., 2005. *BTi Mol. Biol.*, 8–13.
- Höök, F., Rodahl, M., Fredriksson, C., Brzezinski, P., Keller, C.A., Voinova, M., Krozer, A., Kasemo, B., 1997. *Faraday Discuss.* 107, 224–229.
- Komiyama, M., Takeuchi, T., Mukawa, T., Asanuma, H., 2003. *Molecular Imprinting: From Fundamentals to Applications.* Wiley-VCH.
- Li, X., Husson, S.M., 2006. *Biosens. Bioelectron.* 22, 336–348.
- Piacham, T., Josell, Å., Arwin, H., Prachayasittikul, V., Ye, L., 2005. *Anal. Chim. Acta* 536, 191–196.
- Priego-Capote, F., Ye, L., Shakil, S., Shamsi, S.A., Nilsson, S., in press. *Anal. Chem.*
- Risveden, K., Pontén, J.F., Calander, N., Willander, M., Danielsson, B., 2007a. *Biosens. Bioelectron.* 22, 3105–3112.
- Risveden, K., Bhand, S., Pontén, J.F., Andén, T., Calander, N., Willander, M., Danielsson, B., 2007b. *Sens. Actuat. B.* 127, 198–203.
- Sallacan, N., Zayats, M., Bourenko, T., Kharitonov, A.B., Willner, I., 2002. *Anal. Chem.* 74, 702–712.
- Sauerbrey, Z., 1959. *Z. Phys.* 155, 206–222.
- Sellergren, B. (Ed.), 2001. *Molecularly Imprinted Polymers: Man-made Mimics of Antibodies and their Applications in Analytical Chemistry.* Elsevier.
- Surugi, I., Danielsson, B., Ye, L., Mosbach, K., Haupt, K., 2001. *Anal. Chem.* 73, 487–491.
- Voinova, M.V., Jonson, M., Kasemo, B., 1997. *J. Phys.: Condens. Mat.* 9, 7799–7808.
- Yan, M., Ramström, O. (Eds.), 2005. *Molecularly Imprinted Materials: Science and Technology.* Marcel Dekker.
- Ye, L., Cormack, P.A.G., Mosbach, K., 2001. *Anal. Chim. Acta* 435, 187–196.
- Ye, L., Surugi, I., Haupt, K., 2002. *Anal. Chem.* 74, 959–964.
- Yoshimatsu, K., Reimhult, K., Krozer, A., Mosbach, K., Sode, K., Ye, L., 2007. *Anal. Chim. Acta* 584, 112–121.